ISSN 2176-5480

22nd International Congress of Mechanical Engineering (COBEM 2013)
November 3-7, 2013, Ribeirão Preto, SP, Brazil


# APPROXIMATED ENTROPY ALGORITHM APPLIED TO THE CHARACTERIZATION OF THE VIBRATION OF CRACKED SHAFTS

**Diego Luchesi Sampaio**
**Rodrigo Nicoletti**
University of São Paulo, São Carlos School of Engineering, Trabalhador São Carlense 400, 13566-590 São Carlos, Brazil
diegolsampaio@yahoo.com.br, rnicolet@sc.usp.br

***Abstract.*** *Signal analysis based on entropy calculation has been successfully applied in different areas of science, as biology and medicine, for the characterization of the irregularity and complexity of data and extraction of relevant information for the identification of failures and anomalies. The Approximated Entropy (ApEn) is known for being able to classify complex systems with small data sets and a good robustness to noise. The presence of cracks in rotating machinery shafts is a problem which has been studied throughout the years and no definitive solutions for identification have been found. This paper uses the Approximated Entropy algorithm to analyze the vibration of a Jeffcott rotor during the coast up on the presence of cracks modeled by the Fractal Mechanics and studies the main parameters that affect the system as unbalance, crack geometry and acceleration rate, as well as the parameters which define the entropy technique performance. The results show that the ApEn may be a valuable tool for crack identification and growth monitoring.*

***Keywords:*** *rotor dynamics, crack detection, approximate entropy, identification.*

## 1. INTRODUCTION

Since the 1970s, there has been a growing interest in understanding the dynamics of cracked shafts in the rotating machinery literature. With the increasing importance of the turbo machinery on the electrical power generation and aerospace industry, the appearance of cracks in the shafts of these machines became a concern of mechanical engineering researchers because of the potential catastrophic effects of a failure. According to El Arem and Maitournam (2009), between 1970 and the first years of the 1980s, at least 28 failures due to unidentified cracks were registered in the USA energy industry.

The presence of a crack introduces an additional flexibility to the shaft, which reduces the overall stiffness of the shaft. Such knowledge comes from the 1950s (Dimarogonas, 1996). Several authors dedicated efforts to understand the mechanism of opening and closing of the crack while the shaft rotates, which is commonly referred as the breathing behavior of the crack. Mayes and Davis (1984) suggested that on a system with a rotor lying on bearings, so that the main shaft deflection comes from the weight influence instead of other sources, the crack starts to open when its tip reaches the symmetry axis of the rotor and described this dynamics by a harmonic function. Jun *et al*. (1992) studied the forces in the crack section during the shaft rotation and obtained a crack breathing function by applying the principles of the Fracture Mechanics. Gasch (1993) reviewed the shaft crack literature and proposed a modeling method where the crack acts as a hinge, opening and closing once per revolution, while the stiffness is switched from a normal (no crack) and higher value (closed crack) to a lower value (open crack). Darpe *et al.* (2004) compared the switching and the response dependent breathing behaviors of cracked shafts during coast up and coast down and concluded that the breathing model yields more reliable results when compared to experimental findings. Zhou *et al.* (2005) performed experimental investigations with cracked shafts and found reasonably equivalent results with those theoretically reported by Darpe *et al.* (2004). Al Shudeifat and Butcher (2011) proposed improvements to the work of Mayes and Davis (1984), suggesting that while the cracked shaft rotates its centroid and neutral line, from which the crack starts to open, are constantly repositioned.

Literature in the area provides a good knowledge basis about shaft crack dynamics. As reported by Dimaragonas (1996), it is known that the shaft stiffness reduction causes the critical frequency of the system to be also reduced, but this feature is poorly reliable as long as deep cracks will cause slight changes. Darpe, *et al.* (2004) and Al Shudeifat and Butcher (2011) detected the presence of higher vibration harmonics during shaft rotation. Those harmonics become more noticeable during the passage through subharmonics of the critical frequency, where vibration amplitude peaks can also be noticed depending on the crack depth and other physical characteristics of the system. Complex orbits and orbit phase shifts were also observed by many authors, including Darpe *et al.* (2004), Zhou *et al.* (2005) and Shudeifat and Butcher (2011).

Although the described advances in literature provided ways for cracks identification, this is still a subject of interest in the engineering academy since many of the methods proposed require detailed vibration analysis and eventually may not be adequate for failure prevention when cracks are still incipient. The present work presents a different technique, which emerged from the hypothesis that the Approximate Entropy, successfully employed in some fields of science,

ISSN 2176-5480



could generate relevant information about crack presence and severity, allowing for fast detection and classification during system coast up.

## 2. APPROXIMATE ENTROPY

Approximate Entropy (ApEn) is a statistical index used to quantify the irregularity of a time series (Pincus, 1991) and it was designed "for the data analyst that will distinguish data sets by a measure of regularity" (Pincus, 1994). It has been widely applied by researches in the fields of Medicine and Biology for the characterization of signals, including respiratory pattern investigations during panic disorder (Chen *et al.,* 2005), motion monitoring of young and older humans (Yentes *et al.*, 2012), electroencephalogram comparison of patients with epilepsy absence with health volunteers (Burioka, 2005) and the study of tropical trees sap flow temporal dynamics under water deficit (Souza *et al.*, 2003). In the engineering area, few ApEn usage reports are available, but it was successfully used for machine healthy monitoring and bearing defect detection (Yan and Gao, 2006), and electrical power swing fault detection (Fu *et al.,* 2009).

ApEn may be described as a value that results from a calculation over a set of data points, which estimates the irregularity of the series, with larger values indicating more complex data. The algorithm searches for corresponding patterns within the data set and measures the "likelihood that runs of patterns that are close remain close on the next incremental comparison" (Pincus and Goldberger, 1994), that is, a given number of points m is compared to any other possible m sized array inside the data set and considered correspondent when the maximum distance between two data points is less than a tolerance r. Than the process is repeated to m + 1 and the conditional probability that the runs remain inside the defined range is calculated.

Given a temporal series of N data points, x(n) = x(1), x(2) … x(N), the ApEn can be calculated as follows:

1) Define vectors of size m in the form of Eq. (1):

$$X(i) = [x(i), x(i+1), \ldots x(i+m-1)],\ i = 1 \text{ to } N - m + 1; \tag{1}$$

2) Define $d(X(i), X(j))$ as the maximum absolute difference between two elements of each vector, as described by Eq. (2):

$$d(X(i), X(j)) = \max_{k=0\sim(m-1)} \left[ \left| X(i+k) - X(j+k) \right| \right] \tag{2}$$

3) Compare each possible $X(i)$ vector of size m to all possible $X(j)$ vectors, $j = 1 \text{ to } N - m + 1$, and let $N^m(i)$ be the number of matches where $d(X(i), X(j)) \leq r$ . The $r$ value acts at the same time as a noise filter and a match tolerance, being commonly calculated as a portion ($k$) of the series ($S$) standard deviation ($std$), as shown in Eq. (3):

$$r = k.std(S) \tag{3}$$

4) Calculate the ratio of matches over the total number of vectors, as Eq. (4):

$$C_i^m(r) = \frac{N^m(i)}{N - m + 1} \tag{4}$$

5) Define $\Phi^m(r)$ as Eq. (5):

$$\Phi^m(r) = \frac{1}{N - m + 1} \sum_{i=1}^{N-m+1} lnC^m(i) \tag{5}$$

6) Increase the embedded dimension $m$ to $m + 1$ and repeat steps from 1 to 5 to obtain $\Phi^{m+1}(r)$.

7) The ApEn is calculated by the limit given by Eq. (6):

$$ApEn(m,r) = \lim_{N\to\infty} \left[ \Phi^m(i) - \Phi^{m+1}(i) \right] \tag{6}$$

ISSN 2176-5480



8) In practical applications, when using a finite time series, the ApEn value can be approximated by Eq. (7):

$$ApEn(m,r) = \Phi^{m}(i) - \Phi^{m+1}(i) \tag{7}$$

## 3. CRACKED SHAFT MODEL

The rotor model considered in this work is the Jeffcott's, which is composed of a flexible massless shaft mounted on rigid bearings with a disc of mass *m* assembled in its central position. A crack of depth *a* exists in the mid-span of the shaft. The shaft diameter is *D* and the length is *L*, the eccentricity of the unbalance is given by $\varepsilon$ and the internal damping is *c*. A rotating coordinates system is adopted, where the $\xi$ axis represents weak direction of the crack and the η axis represents the strong direction, as shown in Fig. 1. The angle between the eccentricity and the crack direction is $\beta$ and the shaft rotation angle is $\theta$.

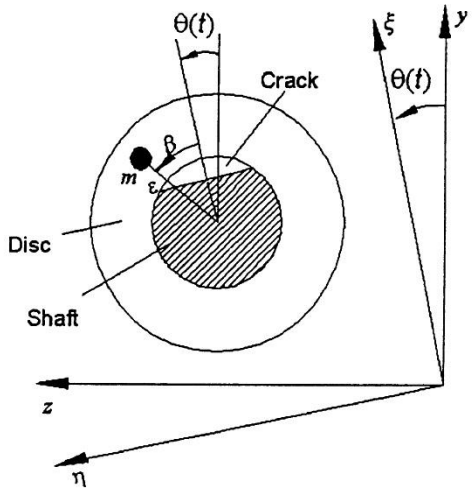


Figure 1 – Rotational and Inertial coordinates (Jun *et al.*, 1992)

In rotating coordinates, the equations of motion of the shaft are expressed as Eq. (8) and Eq. (9). The gravity acceleration is g.

$$m(\ddot{\xi} - 2\dot{\theta}\dot{\eta} - \dot{\theta}^2\xi) - c(\dot{\xi} - \dot{\theta}\eta) + k_{\xi}\xi + k_{\xi\eta}\eta = m\varepsilon\dot{\theta}^2 \cos\beta - mg\cos\theta + m\varepsilon\ddot{\theta}\sin\beta \tag{8}$$

$$m(\ddot{\eta} - 2\dot{\theta}\dot{\xi} - \dot{\theta}^2\eta) - c(\dot{\eta} - \dot{\theta}\xi) + k_{\eta}\eta + k_{\eta\xi}\xi = m\varepsilon\dot{\theta}^2 \sin\beta - mg\sin\theta + m\varepsilon\ddot{\theta}\cos\beta \tag{9}$$

According to Darpe *et al.* (2004) the stiffness coefficients in the rotational coordinates can be obtained from the calculation of the shaft flexibility split into two parts: the normal flexibility plus the flexibility due to the crack presence. The flexibility due to the crack is given by Eq. (10):

$$g_{ij} = \frac{\partial u_i}{\partial Q_j} \tag{10}$$

where i = ξ or η, j = ξ or η and μ is the deflection due to the crack which is given by Eq. (11). $Q_j$ are the forces that act in the section of the crack.

$$\mu_i = \frac{\partial}{\partial Q_j} \int J(\alpha)\, d\alpha \tag{11}$$

J(α) is the energy density function demonstrated in Eq. (12):

$$J(\alpha) = \frac{I}{E}(K^I)^2 \tag{12}$$

ISSN 2176-5480



$K^I$ is the total stress intensity factor (SIF), i.e., the sum of the stress intensity factor in both ξ and η directions, shown in Eq. (13):

$$K^I = K^I_{Q\xi} + K^I_{Q\eta} \tag{13}$$

The stress intensity factor reveals the magnitude of the stress field in a certain point of the cracked section, therefore being function of the value of *w* (shown in Fig. 2), which represents the position along the crack edge. The superscript I in the Stress Intensity Factor denotes the mode I from the three crack modes described by the Fracture Mechanics. The mode I explains the normal opening of the crack, while the two other modes are related to shearing effects.

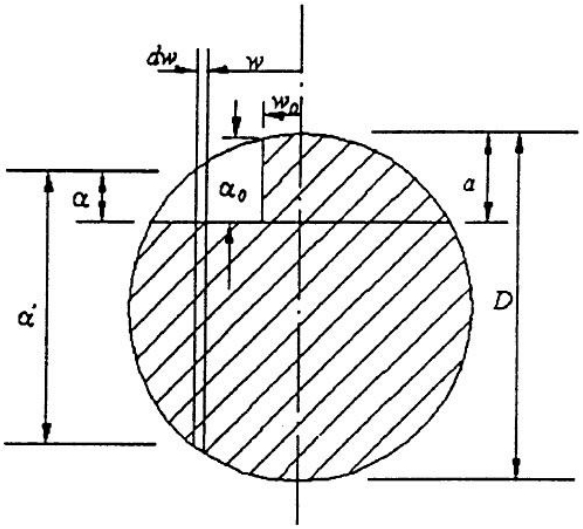


Figure 2 - Cracked section of the shaft with corresponding geometrical parameters (Darpe *et al.*, 2004)

The SIF in each of the directions can be calculated by Eq. (14) and Eq. (15):

$$K^I_{Q\xi} = \sigma_\xi \sqrt{\pi\alpha} F(\alpha/\alpha') \tag{14}$$

$$K^I_{Q\eta} = \sigma_\eta \sqrt{\pi\alpha} F'(\alpha/\alpha') \tag{15}$$

The bending stresses in rotating coordinates, ξ and η, are expressed by Eq. (16) and Eq. (17):

$$\sigma_\xi(w) = \frac{\left(Q_\xi L/4\right)\left(\alpha'/2\right)}{I} \tag{16}$$

$$\sigma_\eta(w) = \frac{\left(Q_\eta L/4\right)w}{I} \tag{17}$$

The functions F and F' are given by the Fracture Mechanics, according to Eq. (18) and Eq. (19):

$$F(\alpha/\alpha') = \sqrt{\frac{2\alpha'}{\pi\alpha}\tan\left(\pi\alpha/2\alpha'\right)}\,\frac{\left\{0.923 + 0.199\left[1 - \sin\left(\pi\alpha/2\alpha'\right)\right]^4\right\}}{\cos\left(\pi\alpha/2\alpha'\right)} \tag{18}$$

$$F'(\alpha/\alpha') = \sqrt{\frac{2\alpha'}{\pi\alpha}\tan\left(\pi\alpha/2\alpha'\right)}\,\frac{\left\{0.752 + 2.02\left(\alpha/\alpha'\right) + 0.37\left[1 - \sin\left(\pi\alpha/2\alpha'\right)\right]^3\right\}}{\cos\left(\pi\alpha/2\alpha'\right)} \tag{19}$$

The inertial moment I is expressed as Eq. (20):

ISSN 2176-5480



$$I = \frac{\pi D^4}{64} \tag{20}$$

The chord α' can be calculated by Eq. (21):

$$\alpha' = \sqrt{D^2 - (2w)^2} \tag{21}$$

The total flexibilities of the shaft in each direction can be obtained by Eq. (11), Eq. (12) and Eq. (13):

$$g_\xi = \frac{L^3}{48EI} + \iint \frac{128L^2\alpha'^2\alpha}{E\pi D^8} F(\alpha/\alpha')^2 d\alpha dw \tag{22}$$

$$g_\eta = \frac{L^3}{48EI} + \iint \frac{512L^2w^2\alpha}{E\pi D^8} F'(\alpha/\alpha')^2 d\alpha dw \tag{23}$$

$$g_{\xi\eta} = g_{\eta\xi} = \iint \frac{256L^2\alpha' w}{E\pi D^8} F(\alpha/\alpha')F'(\alpha/\alpha') d\alpha dw \tag{24}$$

The limits of the integrations will depend on the amount of the crack that is open. As suggested by Jun (1992), the signal of the total SIF can be used to determine the transition between the open and the closed part of the crack in the η direction, while in the ξ direction it is reasonable to assume that the crack is always fully open.

Finally, the stiffness in the direct and cross directions are calculated by Eq. (25), Eq. (26) and Eq. (27):

$$k_\xi = \frac{g_\eta}{g_\xi g_\eta - g_{\xi\eta}^2} \tag{25}$$

$$k_\eta = \frac{g_\xi}{g_\eta g_\xi - g_{\eta\xi}^2} \tag{26}$$

$$k_{\xi\eta} = k_{\eta\xi} = \frac{-g_{\eta\xi}}{g_\xi g_\eta - g_{\xi\eta}^2} \tag{27}$$

To facilitate the parametric study, the following dimensionless parameters are defined:

$$a = a/D, \quad e = \varepsilon/D, \quad \zeta = c/2\sqrt{k_0 m}, \tag{28}$$

## 4. MATERIALS AND METHODS

For obtaining a model simulation of different shaft coast up configurations, Eq. (8) and Eq. (9) were numerically integrated with a time step of 0.00001 s, using second and third order Runge-Kutta methods provided by the MATLAB® software. Each integration was composed of ten time steps, which led to total integration time of 0.0001 s (10 KHz sampling rate). Before each integrating procedure, the shaft stiffness was recalculated through Eq. (14) to Eq. (27) and then assumed constant during 0.0001 s. Displacement values were converted from rotational to inertial coordinates and recorded for later analysis. Due to the influence of the initial transient of the numerical solution, the 10000 first data points of each simulation were discarded.

To facilitate the model comparison with experimental findings, physical parameters adopted for the simulations were based on those reported by Zhou *et al.* (2005) from real testing kits: m = 1.805 Kg, L = 0.22 m and D = 0.01 m. Additional parameters are g = 9.81 m/s$^2$, E = 210 GPa and β = 0 °.

The chosen values for the parameters resulted in a system critical frequency of 507.4 rad/s (4845 rpm) and the 1/2 and 1/3 sub harmonics of 253.7 rad/s (2422.6 rpm) and 169.1 rad/s (1615 rpm), respectively.

The simulations are performed with the following dimensionless parameters: a = 0.1, e = 0.1 and ζ= 0.01. During all test runs, the system is coasted up from 0 to 600 rad/s and, except for the acceleration rate tests, a 100 rad/ s$^2$ rate is

ISSN 2176-5480



employed. The resultant vertical vibration of the shaft was acquired and inputted to the ApEn calculation, as shown in the following section of results.

The ApEn calculation was executed by a code implemented in MATLAB® software.

## 5. RESULTS

### 5.1 ApEn parameter definition

ApEn response is known to be very sensitive to its intrinsic parameters, *m* and *r*, and also to some data parameters as size and sampling rate. Chen *et al.* (2008) demonstrated that a wrong parameter selection can lead a chirp signal to be considered more irregular than a white noise, proving the ApEn relative consistency issue, while Pincus and Goldberger (1994) recognized the variation of the algorithm and recommended that comparisons be done with fixed parameters.

The r value defines the range inside which two m-sized vectors are considered equivalent, working at the same time as the similarity boundary and a noise filter. The *r* value is commonly defined as portion of the standard deviation of the series, so that the algorithm can adequate itself to the amplitude of the data. Using the standard system parameters described in Section 3, a reference signal composed of 1000 data points acquired at 10 KHz, which represents the shaft being accelerated from 200 to 210 rad/s, was employed to a parameter comparison as shown in Fig. 3, where *k* represents a multiplier of the series standard deviation.

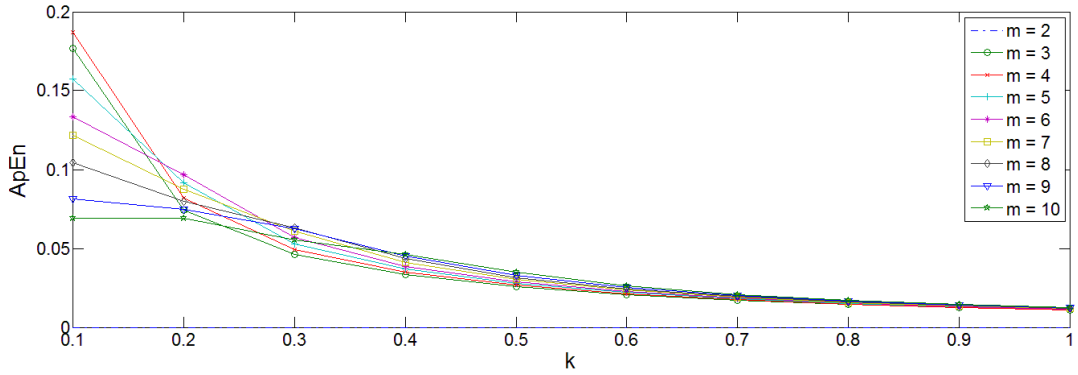


Figure 3 - ApEn for different *m* an *k* values

Even though some authors as Yentes, *et al.* (2012) investigated the possibility of using short data sets, Pincus and Goldberger (1994) recommended that for a good ApEn estimation at least $10^m$ points must be included in the calculation. Therefore, large values of m would require a large number of data points. Although in most engineering applications acquiring large data sets should not be a problem, we would rather work with shorter sets as possible to expose detailed information of the data, thus m = 3 was selected, which led the data sets size to be 1000. Figure 3 shows the ApEn curves for different *m* values along a *k* range from 0.1 to 1. For low values of *k,* the ApEn has an intense variation depending on the m value, so k = 0.5 was selected to be out of the uncertainty region.

### 5.2 Effect of noise addition

In order to understand the influence of signal noise in the resulting value of the ApEn calculus, a Gaussian white noise was added to a reference signal (system parameters described in Section 3) containing 1000 data points that represents the shaft being accelerated from 200 to 210 rad/ $s^2$. The signal-to-noise ratio (SNR) was increased from 0 to 100 dB as shown in Fig. 4. Approximate entropy demonstrates good tolerance to noise and a threshold (60 db) between affected and non-affected values is clearly noticeable. For SNR values below the threshold of 60 dB, the calculated entropy is the noise entropy, whereas for values above the threshold the noise is almost neglected by the method. It is important to understand that the noise threshold depends on the selection of the r value, which acts as filter. This finding indicates that the ApEn may be suitable for application over raw signal data, therefore reducing the processing time.

ISSN 2176-5480



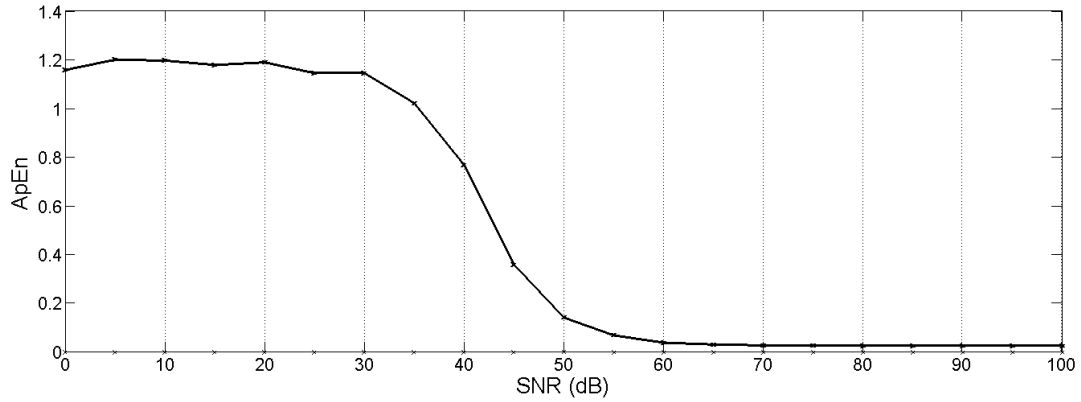


Figure 4 - Effect of noise addition in the ApEn value

### 5.3 Effect of crack depht

Results obtained for different cracks depths (Fig. 5) indicate that, for crack depths over 5% of the shaft diameter, peaks of the ApEn value appear during the passage through the 1/3 and 1/2 subharmonics of the critical speed and both the maximum peak value and width will depend upon the failure depth. As deeper the crack becomes, the higher will be the maximum entropy value and the larger will be the speed range where the peaks exist. Such results can be considered as a reliable indication of the crack depth and it is a potential method for crack growth monitoring. The results also show reasonable accordance with the experimental observations done by Zhou *et al*. (2005), where complex orbits (two circle topology) appears when a crack is present and the speed range where they are present is enlarged by the depth of the crack. Also, Jun et al. (1992), Darpe *et al.* (2004), and Al Shudeifat and Butcher (2011) reported the presence of higher vibration frequencies while crossing the subharmonics of the critical frequencies, which is the reason for the increase in the ApEn value.

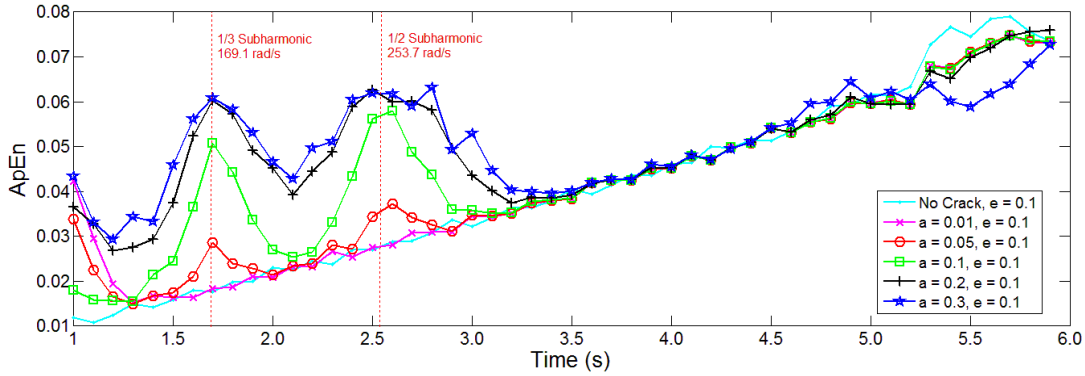


Figure 5 - Effect of crack depth on the ApEn value

### 5.4 Effect of crack depht and umbalance level combined

Figure 6 shows the comparison of the coast up vertical vibration signal ApEn for different configurations of crack depth and unbalance level. When no crack is present, it can be clearly seen that the ApEn value is not affected by simply increasing the unbalance level and the values obtained for e = 0.1 and e = 0.3 are exactly the same. In the presence of a crack, entropy peaks appear during the passage through the 1/3 and 1/2 subharmonics of the critical speed and both the maximum value and the width of the peaks depend on the depth of the failure and the eccentricity of unbalance. An interesting finding is that, for a given value of crack depth, the ApEn is slightly reduced by the increase of the unbalance level, which may be explained by a reduction in the vibration caused by a longer time during which the crack stays open due to the extra force.

ISSN 2176-5480



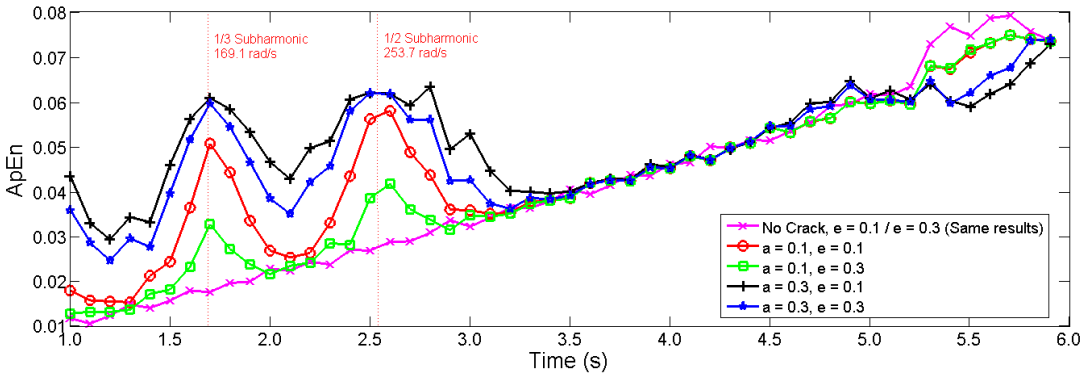


Figure 6 - Effect of crack depth and unbalance level on ApEn

### 5.5 Effect of acceleration

The acceleration rate is a determinant parameter of the vibration behavior during system coast up, thus it is fundamental in the understanding of the ApEn results for crack identification. For most of the simulations shown above, a constant 100 rad/s$^2$ was adopted, which complies with the turbo machinery characteristics. Figure 7 shows the ApEn calculated during shaft coast up for different values of acceleration. It is noticeable that, due to the constant data set size (1000 points) used, lower rates will result in a higher number of calculation points.

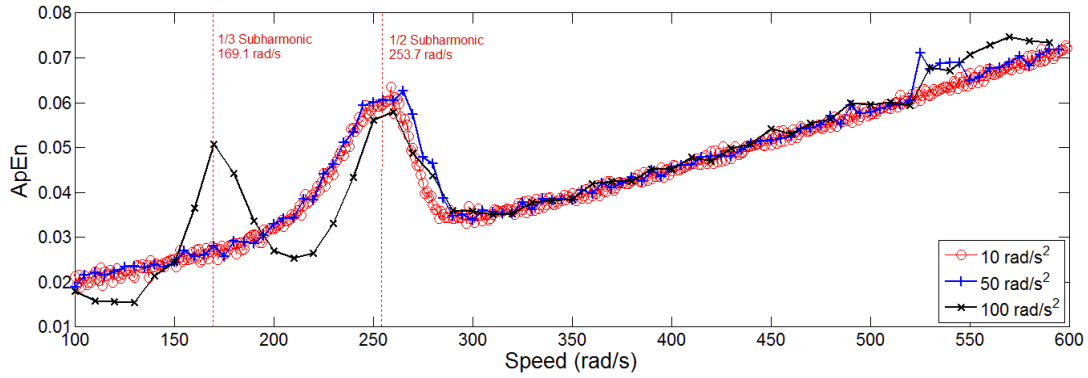


Figure 7 - Effect of the acceleration rate on ApEn

In Figure 7, it is seen an important characteristic when the acceleration rate is lowered: the 1/3 sub harmonic peak disappears. For both 10 rad/s$^2$ and 50 rad/s$^2$ the ApEn has a single peak while crossing the 1/2 sub harmonic, but this peak is even higher and thicker than the one found for 100 rad/s$^2$.

### 5.6 Effect of the internal damping factor

Four levels of internal damping factor were studied from $\zeta = 0.01$ to $\zeta = 0.07$. As shown in Fig. 6, an increase in the damping factor causes the ApEn peak value to be reduced, as should be logically expected as long as a higher damping will lead to a reduction in the vibration power. However, even for the highest damping value, entropy peaks can be noticed while passing through the 1/2 and 1/3 subharmonics of the critical frequency.

ISSN 2176-5480



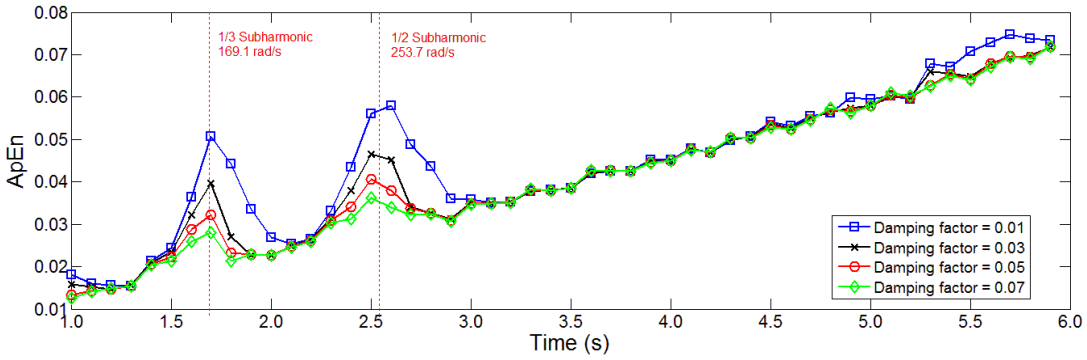


Figure 8 - Effect of damping factor on ApEn

### 5.7 Effect of the β angle

The β angle, between the crack strong direction and the eccentricity, is reknown to influence the vibration response of the cracked shaft. However, as seen in Fig. 9, the approximated entropy is barely affected by the angle change. The 1/2 sub harmonic peak value is slightly increased by the angle increase, while the 1/3 sub harmonic is almost not impacted. This is a positive result, because it indicates that independently of the β angle, the entropy peaks are still reliably related to the crack presence and depth.

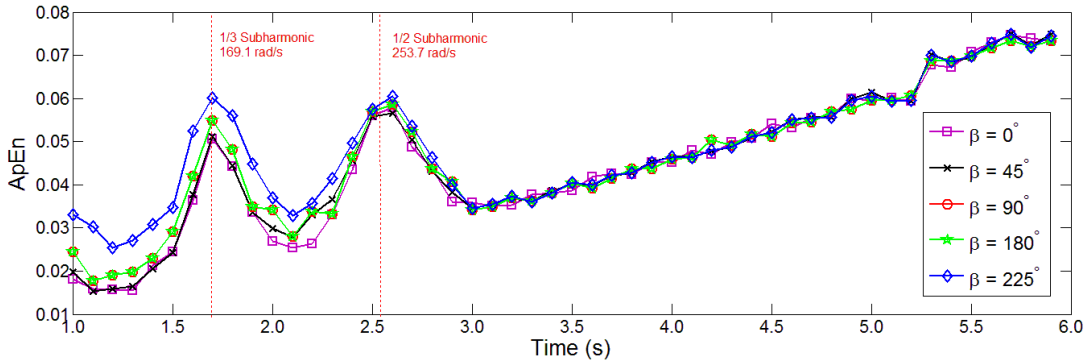


Figura 9 - Effect of the β angle on the ApEn

## 6. CONCLUSIONS

The Approximate Entropy algorithm proved to be a valuable tool for rotating machinery monitoring and shaft crack identification and characterization. Based on previous knowledge and the literature available on both the ApEn calculation and shaft crack dynamics, it was hypothesized that ApEn could provide good information about crack presence and its severity, which could be confirmed by theoretical experimentation. ApEn has known limitations, including its lack of relative consistency and high sensibility to parameters choice, but that could be overcome. The algorithm also demonstrated good tolerance to noise, which implies that it can be applied over raw data, thus reducing processing time. By applying appropriated parameters in the ApEn estimation, entropy peaks could be identified during system coast up, mainly during the passage through the 1/2 and 1/3 sub harmonics of the critical frequency and the method effectiveness was demonstrated for several different system configurations. Results suggest that ApEn could be useful for crack identification and growth monitoring. Finally, the proposed procedure has some advantages over traditional crack detection methods, as orbit and spectral analysis, because it only requires that the vibration be measured in the vertical direction and may be used as an input for automatic classifying systems, discarding the need of human interpretation.

## 7. ACKNOWLEDGEMENT

CNPq (Conselho Nacional de Desenvolvimento Cinentífico e Tecnológico) is acknowledged by the support to this project.

ISSN 2176-5480



## 8. REFERENCES

Al-Shudeifat, M. A. and Butcher, E. A., 2011. "New breathing functions for the transverse breathing crack of the cracked rotor system: Approach for critical and subcritical harmonic analysis", Journal of Sound and Vibration, Volume 330, Issue 3, Pages 526-544.

Burioka N., Cornélissen G., Maegaki Y., Halberg F., Kaplan D.T., Miyata F., Fukuoka Y., Endo M., Suyama H., Tomita Y., Shimizu E., 2005. "Approximate entropyof the electroencephalogram in healthy awake subjects and absence epilepsy patients.", Clinical EEG and neuroscience : official journal of the EEG and Clinical Neuroscience Society (ENCS), Volume 36, Pages 188-193.

Caldirola, D., Bellodi, L. Caumo, A., Migliarese, G. and Perna, G., 2004. "Approximate Entropy of Respiratory Patterns in Panic Disorder", Am J Psichiatry, Volume 1, Issue 1, Pages 79-87.

Chen, X., Solomon, I.C. and Chon K.H., 2005. "Comparison of the use of Approximate entropy and Sample Entropy: Application to Neural Respiratory Signal", Engineering in Medicine and Biology 27th Annual Conference, Shangai, Chicna.

Darpe A.K., Gupta K. and Chawla A., 2004. "Transient response and breathing behaviour of a cracked Jeffcott rotor", Journal of Sound and Vibration, Volume 272, Issues 1–2, Pages 207-243.

Dimarogonas, A. D., 1996. "Vibration of cracked structures: A state of the art review", Engineering Fracture Mechanics, Volume 55, Issue 5, Pages 831-857.

El Arem, S. and Maitournam, H., 2009 "A cracked beam finite element for rotating shaft dynamics and stability analysis", Journal of Mechanics of Materials and Structures, Volume 3, Issue 5, Pages 893-910.

Fu, L., He, Z.Y., Mai, R.K., and Bo, Z.Q, 2009. "Approximate Entropy and its application to fault detection and identification in power swing", Power and Energy Society General Meeting, Calgary, Canada. Pages 1-8.

Gasch, R., 1993. "A Survey Of The Dynamic Behaviour Of A Simple Rotating Shaft With A Transverse Crack", Journal of Sound and Vibration, Volume 160, Issue 2, Pages 313-332.

Jun, O.S., Eun, H.J., Earmme, Y.Y. and Lee, C.W. , 1992. "Modelling and vibration analysis of a simple rotor with a breathing crack", Journal of Sound and Vibration, Volume 155, Issue 2, Pages 273-290.

Lu, S., Chen X., Kanters, J.K., Solomon I.C, Chon K.H., 2008. "Automatic Selection of the Threshold Value r for Approximate Entropy", Transactions on Biomedical Engineering, Volume 55, No. 8, Pages 1966-1972.

Mayes, I.W and Davies, W.G.R, 1984. "Analysis of the response of a multi-rotor-bearing containing a transverse crack in a rotor", Journal of Vibration Acoustics Stress and Reliability in Design-Transactions of the ASME, Volume 106, Issue 1, Pages 139-145.

Pincus, S.M. and Goldberger, A.L.,1994. "Physiological time-series analysis: what does regularity quantify?", The American Journal of Phisiology, Volume 266, Pages 1643-1656.

Pincus, S.M., 1991. "Approximate Entropy as a measure of system complexity", Proceedings of the National Academy of Sciences of The United States of America, Volume 88, Pages 2297-2301.

Souza, G.M., Ribeiro, R.V., Santos, M.G., Ribeiro, H.L., Oliveira, R.F., 2004. "Approximate Entropy as a measure of complexity in sap flow temporal dynamics of two tropical tree species under water deficit", Annals of the Brazilian Academy of Sciences, Volume 76, Pages 625–630.

Zhou, T., Sun, Z. Xu, J. and Weihua H., 2005. "Experimental analysis of Cracked Rotor", Jornal of Dynamaic Systems, Measurement and Control, Volume 127, Pages 313-320.

Yan, R. and Gao, R.X., 2006. "Approximate Entropy as a diagnostic tool for machine health monitoring", Mechanical Systems and Signal Processing, Volume 27, Pages 824-839.

Yentes, J.M., Hunt, N., Schmid, K.K., Kaipust, J.P, Mcgrath, D. and Stergiou, N., 2012. "Appropriate use of the Approximate Entropy with short data sets", 2013. Annals of Biomedical Engineering, Volume 41, Pages 349-365.

## 9. RESPONSIBILITY NOTICE

The authors are the only responsible for the printed material included in this paper.